ACS Partner Journal

ENVIRONMENT & HEALTH

Open Access

pubs.acs.org/EnvHealth

Article

Pseudomonas aeruginosa Activates the NOD-like Receptor Signaling Pathway by Targeting Nasopharyngeal Cells throughout the Whole Respiratory Tract

Caiqing Peng, Guiying Li, Linghui Peng, Xi Fu, and Taicheng An*

Cite This: https://doi.org/10.1021/envhealth.5c00063

Read Online

ACCESS | Metrics & More | Article Recommendations | Supporting Information

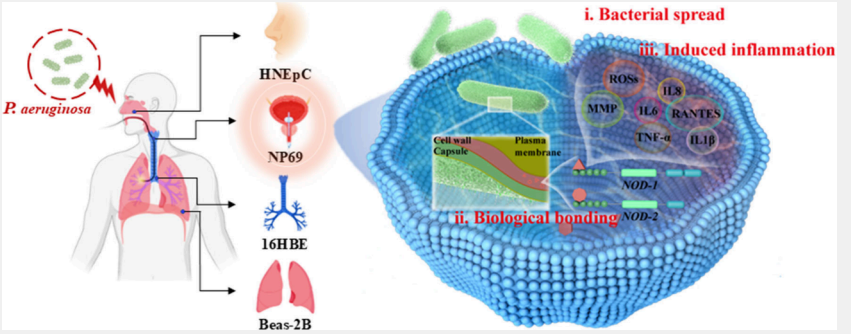

ABSTRACT: Bioaerosols are commonly present in air, and the exposure of bacteria in bioaerosols may lead to allergic reactions and respiratory diseases. However, precise mechanisms underlying the impact of pathogenic bacteria on respiratory health remain poorly understood, and their primary target cells in respiratory tract have not been identified. We systematically explored cytotoxicity of *Pseudomonas aeruginosa* (*P. aeruginosa*) on the whole epithelial cell lines representing different segments of the respiratory tract, including HNEpC (nasal mucosa), NP69 (nasopharynx), 16HBE (bronchus), and Beas-2B (lung) cells. By tracing the entire process of exposure to *P. aeruginosa*, NP69 cells emerged as the primary target, with HNEpC cells showing the lowest susceptibility among the four respiratory cell types. *P. aeruginosa* was transmitted from extracellular space to intracellular region of NP69 cells, accompanied by significant up-regulation (1.5−26.5 fold) of *NOD2* expression, an RNA molecule that specifically binds to bacterial cell walls. Furthermore, cell proliferation activity decreased by 6.8%−46.1%, while levels of inflammatory cytokine interleukin IL-6 and IL-1β increased by 14.5%−181.0% and 50.2%−238.2%, respectively, following intracellular transition of bacteria in NP69 cells. The changes in epithelial-mesenchymal transition (EMT) marker expression at genetic and protein levels and enhancement of functional phenotypes (migratory capacity) confirmed the potential of *P. aeruginosa* to induce malignant transformation of epithelial cells by activating the NOD-like receptor signaling pathway. This comprehensive examination of comparative cytotoxicity of bacteria on cells throughout the human respiratory tract elucidates specific target cells and damage mechanisms, offering valuable insights into health risk assessment, risk prevention, and bacteria control.

KEYWORDS: *Bacteria, Pathogen, Respiratory exposure risk, Cellular targeting, NOD-Like receptor signaling pathway*

1. INTRODUCTION

Bioaerosols are ubiquitous in environment, with diverse and complex sources, including nature like leaves and mold growth on wet sites.[1,2] Moreover, bioaerosols are produced from human activities and contain a wide variety of bacterial species.[2,3] Bacterial aerosols have been frequently detected in municipal landfills, sewage treatment, organic waste processing and agriculture; indoor locations with suitable environmental conditions, such as showers and medical facilities; and via daily activities of cooking, cleaning, and exercise.[4−7] Human exposure to bacteria is a particular health concern in densely populated countries like China and India.[8] Among them, the opportunistic pathogenic bacterium *Pseudomonas aeruginosa* (*P. aeruginosa*) is the dominant pathogen, and a significant level of contamination is associated with respiratory tract exposure and infection.[9−11]

Respiratory exposure and infection with *P. aeruginosa* can lead to various human health complications, including bronchiectasis,[12] pneumonia,[13] and chronic obstructive pulmonary disease.[14] Furthermore, *P. aeruginosa* is a main pathogen in respiratory tracts of patients with cystic fibrosis.[15]

Received: March 5, 2025
Revised: August 1, 2025
Accepted: September 2, 2025

Exposure and infection with it in individuals with immunosuppression, allergies, or respiratory diseases may pose additional health risks.[16−18] These vulnerable groups must be taken into account, as they represent approximately one-third of the global population.[1] Therefore, respiratory exposure to *P. aeruginosa* is particularly dangerous, requiring comprehensive assessments of the associated health risks. Numerous clinical studies demonstrate that patients with respiratory colonization of *P. aeruginosa* have an increased risk of moderate to severe respiratory system health problems.[12] *P. aeruginosa* can also induce cell apoptosis[19] and cause lung inflammation in mice.[20] However, the entire process and molecular mechanisms of *P. aeruginosa* from the origin of respiratory exposure to the end point of inflammatory disease induction are lacking.

The attack target and point of infection of bacteria in respiratory tract are most likely to be respiratory epithelial cells; however, given the complex, interrelated anatomical features and clearance mechanisms in mammals, respiratory damage may also spread between respiratory organs.[21] As reported, bacterial aerosols can deposit in the head airway of the respiratory tract by gravity sedimentation and impact, and also diffuse into the lower airway.[22] Movement and propagation of bioaerosols in respiratory tract have been demonstrated through models of computational fluid dynamics,[23] indicating that bacteria can remain throughout the human respiratory tract following inhalation. However, toxic effect variations of exposure to bacteria in different parts of the respiratory tract have not been elucidated and the main attack targets in the respiratory tract have not yet been identified.

Here, *P. aeruginosa* is taken as a representative pathogen due to its wide environmental adaptability, stable survivability in bioaerosols,[24] and as a "High group" in the WHO Bacterial Priority Pathogens List, 2024 (https://www.who.int/publications/i/item/9789240093461). Its uniqueness lies in its advantage of environmental survival in low-nutrition and high-humidity aerosols, and its high detection rate in bioaerosols in scenarios including municipal landfills,[25] wastewater treatment plants,[26] and hospital intensive care units.[27] Cells from nasal (HNEpC), nasopharyngeal (NP69), bronchial (16HBE), and lung (Beas-2B) regions were used as experimental models of exposure to explore exposure and attack target cells throughout the respiratory tract. Transmission of *P. aeruginosa* from extracellular to intracellular space was quantified, and cellular receptors that recognize and bind to bacteria were screened. Cytotoxicity mechanisms, including damage to cell proliferation, mitochondria, inflammation, and chemotaxis, of *P. aeruginosa* were compared among respiratory epithelial cell lines. A mechanism by *P. aeruginosa* to cause respiratory disease through activating an inflammation-related signaling pathway was proposed. The health risks evaluated in this study are applicable to high-risk scenarios such as medical facilities, sewage treatment facilities, and damp and enclosed buildings. It provides supporting evidence for the health risks of pathogens and has methodological transfer value for studying the environmental health effects of other Gram-negative bacteria and similar pathogens.

2. MATERIALS AND METHODS

2.1. Cell Lines, Bacterial Strain, Cultivation, and Exposure

All the cell lines, bacterial strains, and cultivation information are described in Text S1 in the Supporting Information.

The cell culture medium without *P. aeruginosa* was used as the blank control. The exposure concentrations of *P. aeruginosa* were 10, 10^2, 10^3, 10^4, 10^5 CFU/mL, each exposed for 6 h, based on the sampling concentration range of bacterial aerosol in sewage treatment plants[28,29] and the determined proliferative toxicity of respiratory cells. It aims to simulate acute high-concentration exposure scenarios (e.g., aerosol release in medical operations or industrial accidents), which helps to understand the interaction between *P. aeruginosa* and respiratory epithelial cells, independent of the specific transmission route of the bacteria.

2.2. Cellular Adhesion and Gentamicin Selection

The quantitative adherence and invasion of *P. aeruginosa* were measured according to Lamari's method.[30] Briefly, after bacteria exposure, cells were treated with phosphate-buffered saline (PBS) containing 0.5% sodium dodecyl sulfate (SDS) for 5 min for fully lysis. Bacterial number was calculated by the agar plate colony counting method (CFU assay). The bacterial number in the lysate was denoted as W, which is the sum of adhesion and invasion bacteria.

A gentamicin selection assay was used to quantify bacteria invading the cells. Specifically, after exposure to bacteria, cells were treated with 100 μg/mL gentamicin for 1 h to remove extracellular bacteria and then treated with PBS containing 0.5% SDS for 5 min to fully lyse the cells. The bacterial number in lysate was counted to reflect the bacterial number invading the cells, which is denoted as $W1$.

The adhered bacterial number was calculated as the sum of the number of adhesion bacteria and invasion bacteria minus the number of invasion bacteria, which is referred to as $W2$ ($W - W1$). More details are given in Text S2 in the Supporting Information.

2.3. Fluorescein Isothiocyanate (FITC)-Dextran Translocation Assay

Cells were cultured in a 24-well Transwell plate. After the bacteria were exposed and the supernatant was removed, the residual culture medium was washed with sterile PBS. Phenol-free medium (200 μL) containing 0.5 mg/mL FITC-dextran was added to the upper chamber of Transwell, and phenol-free medium (600 μL) without FITC-dextran was added to the lower chamber. Then the mixture was incubated at 37 °C in darkness for 60 min. Take 100 μL of solution from each chamber and measure fluorescence intensity using a microplate reader (Em/Ex = 485 nm/535 nm).

2.4. Cell Viability and Mitochondrial Damage Detection

Proliferation toxicity of bacteria on the respiratory tract cells was measured using a real-time unlabeled cell analyzer (RTCA USA, ACEA Biosciences). Cell impedance detection sensor system was used to track cell morphology, proliferation, and differentiation in real time, integrating microelectrode array at the bottom of hole of the culture plate to obtain cell growth curve. Intracellular reactive oxygen species (ROSs) content were measured with MitoSOX Red mitochondrial superoxide indicator after 6 h of bacterial exposure. Mitochondrial membrane potential (MMP) was measured using a JC-1 assay kit (Beyotime Biotechnology). The details are given in Text S3 in the Supporting Information.

2.5. Enzyme-Linked Immunosorbent Assay

Levels of proinflammatory factors IL-6, IL-1β, tumor necrosis factor TNF-α, and chemokine IL-8 were detected using respective enzyme-linked immunosorbent assay kits (Elabscience Biotechnology). Cytokine levels were measured using cellular supernatant after bacteria exposure, as detailed in Text S4 in the Supporting Information.

2.6. RNA Extraction and Gene Expression Quantification

Cells were cultured in 6-well plates, and total RNA was extracted with Trizol reagent following bacteria exposure. RNA concentration was determined with Nanodrop spectrophotometer (Thermo Fisher Scientific), as detailed in Text S5 in the Supporting Information.

Using the extracted RNA as a template, cDNA was obtained with reverse-transcription kit MonScript RTIII All-in-one Mix with dsDNase. Using the obtained cDNA as template, the MonAmp ChemoHS qPCR Mix kit was used for real-time quantitative polymerase chain reaction to amplify cDNA (the entire experiment was performed in darkness). *Rps18* was used as the reference gene for

https://doi.org/10.1021/envhealth.5c00063
Environ. Health XXXX, XXX, XXX−XXX

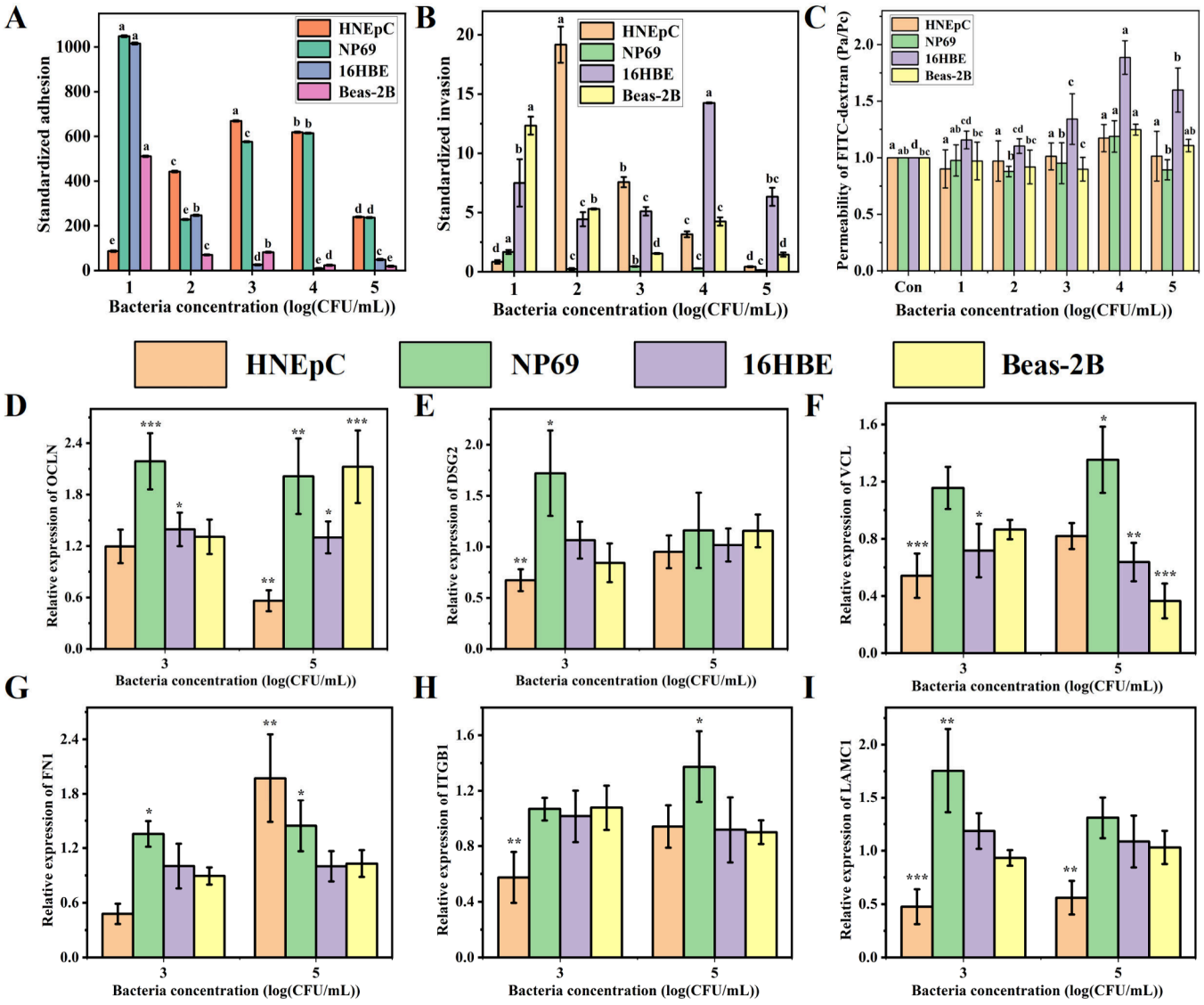

Figure 1. Adhesion and invasion of bacteria toward different respiratory epithelial cells after exposure for 6 h: (A) adhesion efficiency and (B) invasion efficiency of *P. aeruginosa*; (C) the permeability of epithelial cells to FITC-Dextran; expression levels of genes (D) *OCLN*, (E) *DSG2*, (F) *VCL*, (G) *FN1*, (H) *ITGB1*, and (I) *LAMC1* related to in tight intercellular junctions and adhesion in respiratory tract cells. In panels (A)−(C), the sample size is $n = 3$; in panels (D)−(I), the sample size is $n = 4$.

all of the cells. All primers listed in Table S1 were synthesized by Beijing Tsingke Biotech Co., Ltd. Relative gene expression was calculated using the Livak' method.[31]

2.7. Total Protein Extraction and Western Blotting Detection

Cells were cultured in 6-well plates, and total proteins were extracted using Cell Lysis Buffer for Western and IP reagents after bacterial exposure. The protein concentration was determined using BCA Protein Assay Kit, as detailed in Text S6 in the Supporting Information.

The extracted proteins were electrophoresis, membrane transfer, and an antigen−antibody immune reaction. Then, luminescence was identified using horseradish peroxidase-ECL luminescence method with a fully automatic chemiluminescence image analyzer (Shanghai, Tanon-5200CE). The target protein bands were normalized by using ImageJ software. GAPDH and Lamin B were selected as house-keeping proteins for epithelial cells. All the antibodies were from Jiangsu Affinity Biosciences Research Center Co., Ltd. as listed in Table S2 in the Supporting Information.

2.8. Wound-Healing Assay

Cells were cultured in 6-well plates. Before bacteria exposure, a "cross-shaped" symbol was scratched on cells in a Petri dish using a pipet. The scratch was washed with PBS to remove residues, and photographs were taken using an inverted microscope to record the width of the scratch before exposure, which was denoted as B_0. After bacteria were exposed for 6 h, photos were taken to monitor the extent of wound closure, and the width of the scratch was recorded as B_t. The cell migration rate $= \frac{(B_0 - B_t)}{B_0}$.

2.9. Statistical Analysis

All experiments were repeated three times, and results were presented as average ± standard deviation in general. Detailed statistical analysis is given in Text S6 in the Supporting Information.

3. RESULTS AND DISCUSSION

3.1. Transmission of Bacteria to Respiratory Tract Cells

Bacterial adhesion onto cells is the first and key step for pathogens to exert their pathogenicity and induce cytotox-

https://doi.org/10.1021/envhealth.5c00063
Environ. Health XXXX, XXX, XXX−XXX

icity.[32,33] The bacterial spread efficiency from suspension to cellular surface was measured by counting the ratio of the number of bacteria adhering to the cell surface to the total number of introduced bacteria. At *P. aeruginosa* exposure concentration of 10−10^5 colony-forming units (CFU)/mL for 6 h, adhesion efficiencies of bacteria to respiratory epithelial cells were 86.9−669.1, 228.1−1048.3, 8.9−1015.8, and 18.9−511.0 for HNEpC, NP69, 16HBE, and Beas-2B cells, respectively (see Figure 1A). That is, adhered bacterial concentrations were higher than the exposure concentrations, indicating that bacteria proliferated during exposure as the host cells or culture medium provided nutrients for bacteria. Furthermore, bacteria exhibited much greater adhesion efficiency onto the upper (HNEpC and NP69) than to the lower respiratory tract cells (16HBE and Beas-2B). Thus, in the first step of infection, *P. aeruginosa* specifically and selectively adhered onto epithelial respiratory cells in the following order: HNEpC > NP69 > 16HBE > Beas-2B.

Bacteria are capable of invading and replicating in multiple cell types, leading to chronic infections and chronic inflammation.[34] Therefore, bacterial spread efficiency from the cellular surface into cells was measured by counting the ratio of bacterial number inside these cells to introduced bacteria number (Figure 1B). *P. aeruginosa* was detected inside all cell lines, indicating the successful bacterial invasion of host. At bacteria exposure concentrations of 10−10^5 CFU/mL, bacterial invasion efficiency reached 0.4−19.2, 0.1−1.7, 4.4−14.3, and 1.5−12.3 for HNEpC, NP69, 16HBE, and Beas-2B cells, respectively. Therefore, the invading bacterial number was much less than that of adhesion bacteria, because adhesion is a major prerequisite of bacterial invasion. The adhesion bacteria translocate directly from the respiratory cell membrane surface to the cytoplasmic matrix via cellular receptors or bacterial proteins. Invasion ability of bacteria to lower respiratory tract cells was higher than that of upper respiratory tract cells. Rearrangement of actin cytoskeleton in respiratory tract cells occurs during bacterial invasion,[35] dysregulating the normal cell growth and metabolism of these cells.

Bacterial invasion of epithelial barrier mainly occurs through paracellular pathway (penetration through intercellular gaps).[36] We hypothesized that, in NP69 cells, higher bacterial adhesion strengthens cellular physical barriers, hindering membrane penetration, whereas a relatively lower bacterial number invaded these cells than other tested cells. Therefore, we evaluated paracellular permeability by measuring the transport amount of FITC-dextran from the apical side to basal side of epithelium. After exposure to bacteria at 10−10^5 CFU/mL, permeability of FITC-dextran in epithelial cells from the upper to lower respiratory tract was sequentially 90.1%−117.3%, 87.8%−118.9%, 110.3%−188.5%, and 89.9%−124.8% (Figure 1C), indicating that the permeability of epithelial cells could be ranked as follows: 16HBE > Beas-2B > HNEpC > NP69. After bacterial exposure, NP69 cells exhibited the least reduction in permeability, with their physical barriers remaining the most intact. Consequently, this impeded bacterial invasion, validating our hypothesis.

To further clear changes in cell permeability, expression levels of genes involved in tight intercellular junctions that directly regulate intercellular permeability by closing intercellular gaps in respiratory cells,[37] and adhesion molecules that enhance the integrity of epithelial cells by stabilizing cell−cell and cell-matrix interactions[38] in respiratory tract cells, were compared before and after exposure at low and high exposure concentrations (10^3 and 10^5 CFU/mL). As presented in Figure 1D, the expression of *OCLN* (regulating tight junction paracellular permeability barrier) up-regulated by 1.2-(HNEpC), 2.2- (NP69), 1.4- (16HBE), and 1.3-fold (Beas-2B) in these cells after exposure to 10^3 CFU/mL bacteria. However, *OCLN* expression in HNEpC cells down-regulated by 0.6-time ($p < 0.01$) and up-regulated by 2.0-, 1.3-, and 2.1-time ($p < 0.05$) in NP69, 16HBE, and Beas-2B cells, respectively, after exposure to 10^5 CFU/mL bacteria. After NP69 cells being exposed to 10^3 and 10^5 CFU/mL bacteria, *DSG2* (regulating intercellular junction calcium-binding transmembrane glycoprotein) up-regulated by 1.7- and 1.2-time, respectively (Figure 1E); and *VCL* (regulating cell−cell and cell-matrix junctions) up-regulated by 1.2 and 1.4 times ($p < 0.05$), respectively (Figure 1F). *DSG2* and *VCL* in other cell types up-regulated by <1.2-fold or even down-regulated in some cases. The genes *OCLN*, *DSG2*, and *VCL* (regulating tight intercellular junctions) were up-regulated most significantly in NP69 cells, indicating that NP69 cells enhance cell−cell/matrix adhesion, thereby restricting bacterial invasion through the paracellular pathway. Furthermore, after exposure to 10^3 CFU/mL bacteria, *FNI* (regulating cell adhesion and migration) in HNEpC and NP69 cells down-regulated by 0.5 times and up-regulated by 1.4 times ($p < 0.05$), respectively (Figure 1G). After exposure to 10^5 CFU/mL bacteria, *FNI* up-regulated by 2.0 and 1.4 times in HNEpC and NP69 cells, respectively, but changed slightly in other two cell lines. Two other adhesion regulatory genes, *ITGB1* (Figure 1H) and *LAMC1* (Figure 1I), upregulated the greatest expression in NP69 cells after exposure to high and low bacterial concentrations. Therefore, genes regulating tight intercellular junctions (*FN1* and *LAMC1*) and enhancing cell adhesion to extracellular matrix indirectly maintaining integrity of epithelial barrier (*ITGB1*) were the most significantly up-regulated genes in NP69 cells, suggesting that cells prevent bacterial invasion by directly and indirectly forming an intercellular adhesion barrier. Overall, these findings could explain phenomenon of high adhesion but low invasion of NP69 cells, given that these cells appear to form two physical barriers to prevent bacterial invasion involving tight-junction paracellular permeability and intercellular adhesion.

Generally, the first step of *P. aeruginosa* exposure and infection involves transmission of bacterium from extracellular suspension to cell surface via adhesion, and the second step involves invasion from the cellular surface to the interior. Throughout the respiratory tract, the number of *P. aeruginosa* transmitted to the surface of HNEpC and NP69 cells was the highest, whereas the bacterial number in NP69 cells was not the highest among the four cell types due to formation of paracellular and intercellular barriers as a defense response. That is, the number of deposited *P. aeruginosa* in the entire respiratory tract was the highest in the nose and nasopharynx, corresponding with the wide use of nasal and throat swabs for sampling respiratory pathogens.

3.2. Expression Regulation of Cellular Pattern Recognition Receptors Exposed to Bacteria

Bacteria specifically bind to host cellular receptors, initiating signal transduction to further induce cytotoxicity.[39] Therefore, gene expressions of two families of bacterial-based pattern recognition receptors, including NOD-like receptors (NLRs) and Toll-like receptors (TLRs)[40] were analyzed. Among NLR

https://doi.org/10.1021/envhealth.5c00063
Environ. Health XXXX, XXX, XXX−XXX

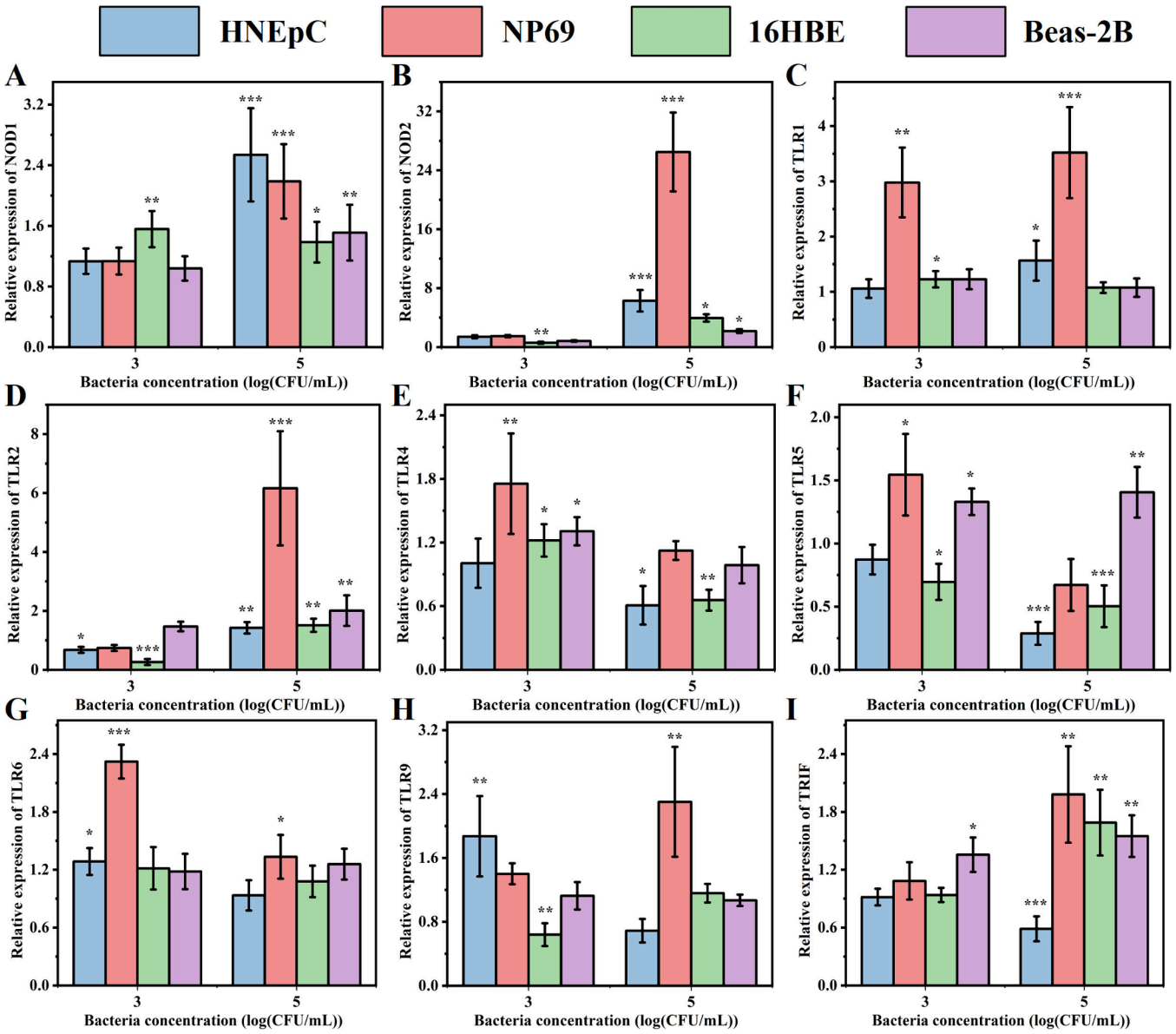

Figure 2. Expression levels of pattern recognition receptor-related genes in human respiratory epithelial cells. Expression levels of gene (A) *NOD1*, (B) *NOD2*, (C) *TLR1*, (D) *TLR2*, (E) *TLR4*, (F) *TLR5*, (G) *TLR6*, (H) *TLR9*, and (I) *TRIF*. Sample size: $n = 4$; statistical method: two-way ANOVA, followed by Dunnett's t-test.

family genes, expression of *NOD1* up-regulated by 1.1-, 1.1-, 1.6-, and 1.0-fold in HNEpC, NP69, 16HBE, and Beas-2B cells, respectively, after exposure to 10^3 CFU/mL bacteria; and it up-regulated by 2.5-, 2.2-, 1.4-, and 1.5-fold ($p < 0.05$), respectively, after exposure to 10^5 CFU/mL (Figure 2A). *NOD2* up-regulated by 1.4- and 1.5-fold in HNEpC and NP69 cells, respectively, but down-regulated by 0.6 and 0.8 times in 16HBE and Beas-2B cells, respectively, after exposure to 10^3 CFU/mL; conversely, it up-regulated in all four cell lines by 6.3, 26.5, 3.9, and 2.2 times ($p < 0.05$), respectively, with the exposure of 10^5 CFU/mL bacteria. That is, the expression level of *NOD2* in NP69 cells was much higher than that in other cell lines (Figure 2B), indicating that respiratory tract cells mainly adhere to*P. aeruginosa* through the binding of intracellular receptors *NOD1* and *NOD2* to diaminopigelic acid and muramyl dipeptide (MDP)[41,42] of bacterial cell wall. Among the four tested cell lines, NP69 cells had the strongest binding ability to bacterial MDP by activating the *NOD2* gene, followed by HNEpC, 16HBE, and Beas-2B cells.

Among TLRs gene family members, the expression of *TLR1* in NP69 cells up-regulated by 3.0- and 3.5-fold ($p < 0.05$) after exposure to 10^3 and 10^5 CFU/mL bacteria, respectively; whereas it up-regulated by <1.6-fold under low- and high-concentration exposure in other cell types (Figure 2C). Expression of *TLR2* (Figure 2D) and *TLR4* (Figure 2E) up-regulated by 6.2 and 1.1 times in NP69 cells after exposure of 10^5 CFU/mL bacteria. After exposure to 10^3 CFU/mL bacteria, the expression of *TLR5* maximum up-regulated 1.5 times ($p < 0.01$) in NP69 cells, whereas it down-regulated in other three cell lines (Figure 2F). Furthermore, the expression of *TLR6* (Figure 2G) and *TLR9* (Figure 2H) in NP69 cells increased by 2.3 and 1.4 times with exposure to low-concentration bacteria and increased by 1.3 and 2.3 times ($p < 0.05$) with high-concentration exposure, respectively; these genes also exhibited greater levels of expression change in

https://doi.org/10.1021/envhealth.5c00063
Environ. Health XXXX, XXX, XXX−XXX

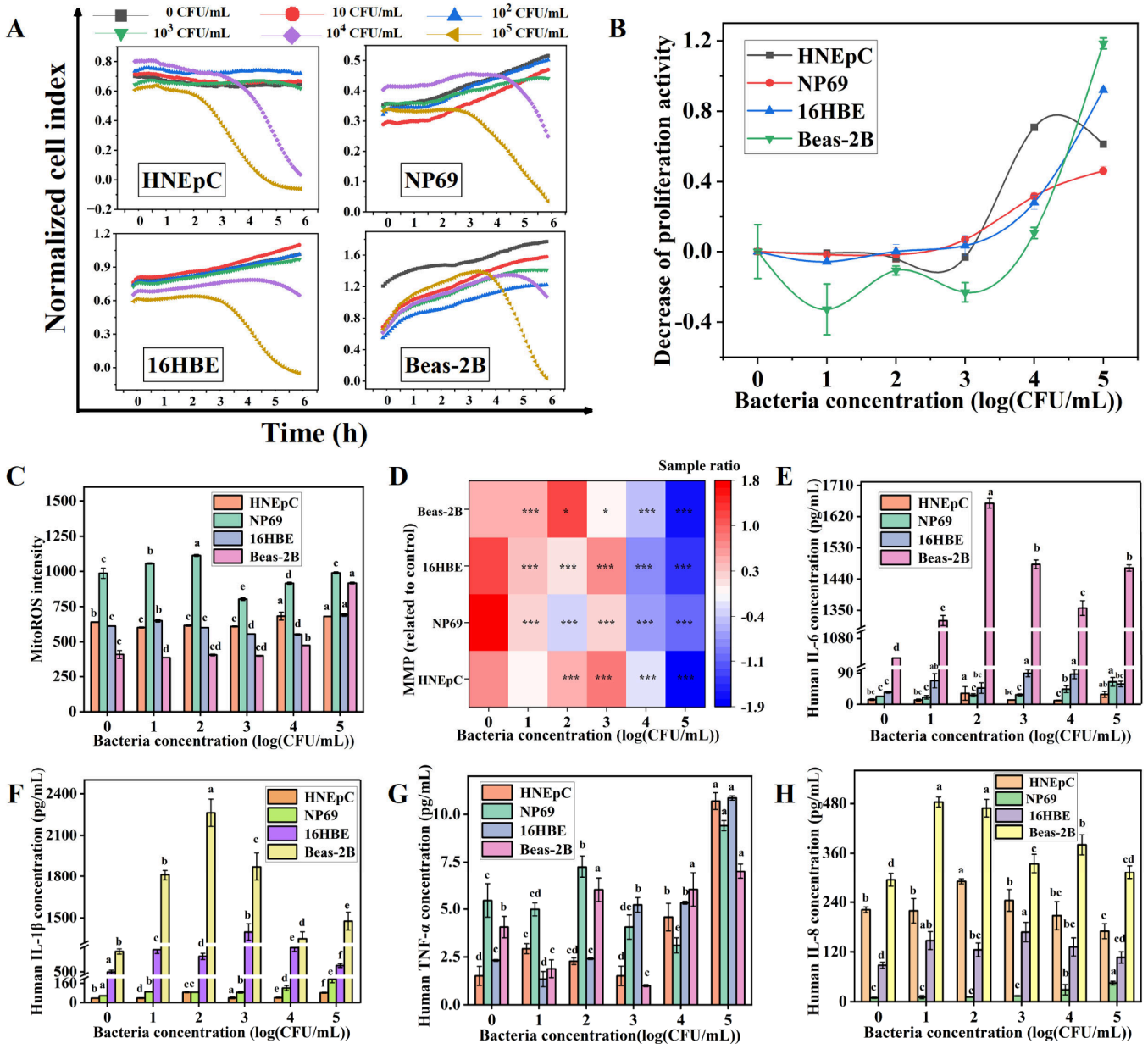

Figure 3. Cytotoxic effects of human respiratory epithelial cells: (A) normalized cell proliferation curve of bacteria after 0−6 h exposure; (B) proliferation activity; (C) the generation of mitochondrial ROSs; (D) heat map of MMP; The concentration of pro-inflammatory factor (E) IL-6, (F) IL-1β, and (G) TNF-α, and the concentration of chemokines (H) IL-8 in cell supernatant. Sample size: n = 3.

NP69 cells than other cell types (Figure 2F). These indicate that respiratory epithelial cells bind to membrane and nucleic acids of *P. aeruginosa*, as *TLR1*, *TLR2*, *TLR4*, *TLR5*, and *TLR6* mainly regulate binding to membrane of pathogenic microorganisms, whereas *TLR9* regulates binding to nucleic acids.[43,44] Additionally, expression of *TRIF* (regulating intracellular signals between TLRs and related signal transduction components) down-regulated by 0.9-time in HNEpC and 16HBE cells, but up-regulated by 1.1 times in NP69 and 1.4 times in Beas-2B cells with exposure to 10^3 CFU/mL bacteria (Figure 2I). With high-exposure concentration, *TRIF* down-regulated by 0.6 times in HNEpC cells, and up-regulated by 1.7, 2.0, and 1.5 times ($p < 0.01$) in 16HBE, NP69, and Beas-2B cells, respectively. Overall, expression of NLRs and TLRs family genes was the most significantly up-regulated in NP69 cells, indicating that NP69 cells have the strongest ability to be recognized and bound by *P. aeruginosa* to activate the innate immune response of respiratory cells.

3.3. Mechanism of Bacteria-Induced Inflammatory Response of Respiratory Cells

3.3.1. Pathogen-Induced Cellular Proliferation Toxicity. The specific binding of host cells to bacteria could induce cytotoxic effects,[45] which can be evaluated by analyzing changes during cellular proliferation. To more intuitively compare toxic effects of bacteria on different respiratory tract cells, cellular proliferation curve at 0−6 h was examined, with 0 being the point at which bacteria was added to cell culture (Figure 3A). During exposure of *P. aeruginosa* at concentrations of 10^4 and 10^5 CFU/mL, proliferation of all cell types slowly increased and then decreased with increasing exposure time, indicating that cells initiate a cooperative defense to overcome toxicity of bacteria given the low bacterial number at

https://doi.org/10.1021/envhealth.5c00063
Environ. Health XXXX, XXX, XXX−XXX

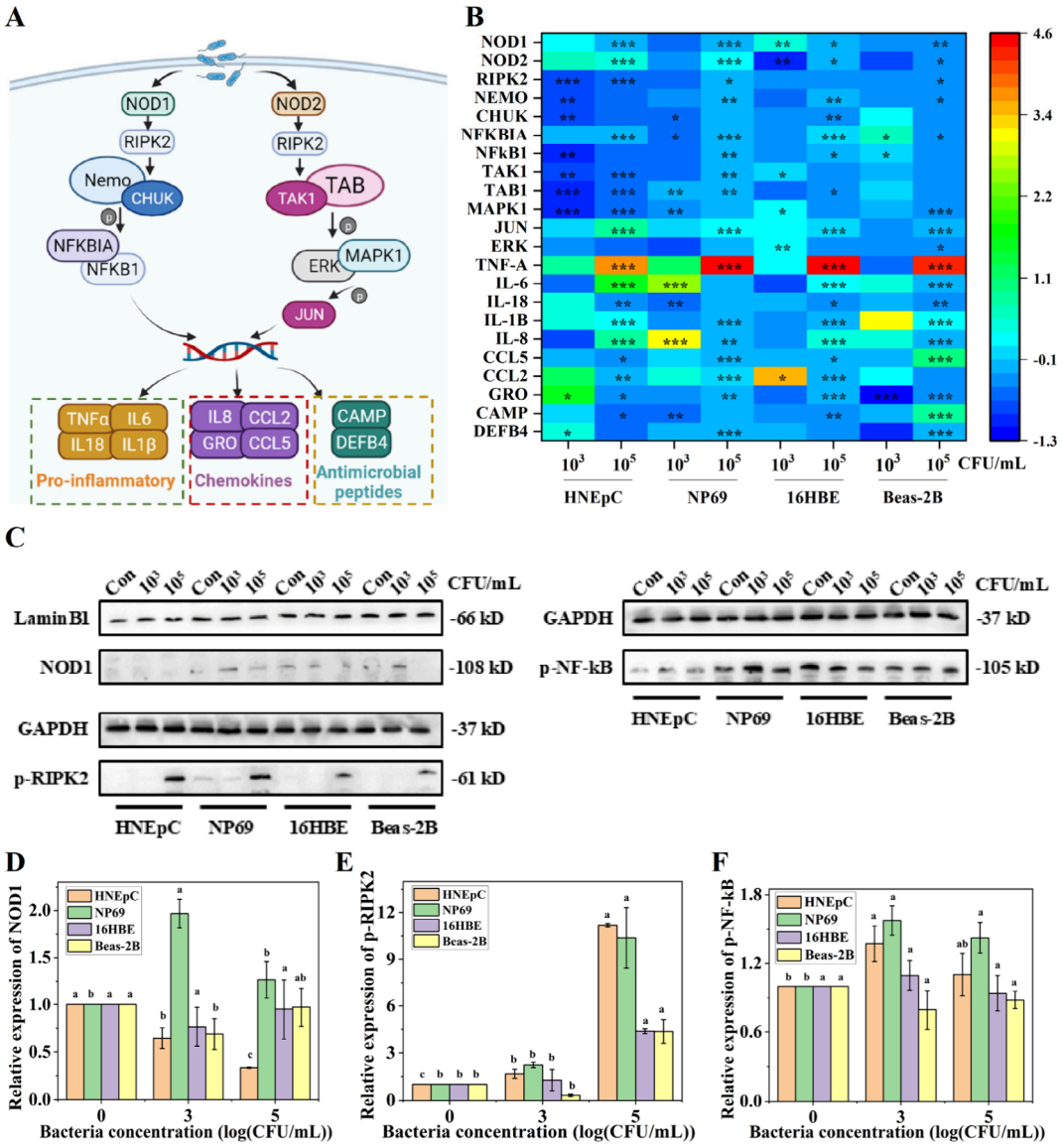

Figure 4. (A) Schematic diagram and (B) gene expression level of NOD-like receptor signaling pathway; (C) the key protein bands detected by Western blotting in the NOD-like receptor signaling pathway; (D–F) relative expression levels of proteins NOD1 (panel (D)), p-RIPK2 (panel (E)), and p-NF-κB (panel (F)). In panel (B), the sample size is $n = 4$; in panels (D)–(F), the sample size is $n = 3$.

the initial exposure stage, enabling cells to continuously proliferate. However, with increasing exposure time, stress of the rapidly proliferating bacteria surpassed the codefense capacity of cells (Figure 1A), resulting in a decline in proliferative activity of respiratory cells. With prolongation exposure time to 18 h (Figure S1A), cellular proliferation showed a similar trend with exposure to 10–10^3 CFU/mL bacteria, possibly due to continuous bacterial proliferation. To deeply reveal specific cellular damage caused by bacteria, proliferation toxicity of *P. aeruginosa* was normalized after 6 h of exposure (Figure 3B). After exposure to 10–10^3 CFU/mL bacteria, the proliferative activity of these cell lines differed insignificantly. However, after exposure to 10^4 CFU/mL bacteria, cellular proliferative activity decreased in the order of HNEpC (70.8%), NP69 (31.7%), 16HBE (28.2%), and Beas-2B (10.6%). With exposure of 10^5 CFU/mL bacteria, cellular proliferation activity decreased in the order of Beas-2B (118.5%), 16HBE (92.0%), HNEpC (61.3%), and NP69 (46.1%). Therefore, the sequence of effects of *P. aeruginosa* exposure on the proliferative activity of four respiratory tract cells varied according to exposure concentration.

To further explore the mechanisms contributing to a decrease of cell proliferation, changes in mitochondrial ROSs and MMP were investigated, as mitochondria are important organelles responsible for cell proliferation and metabolism.[46] The relative ROSs production in HNEpC, NP69, and 16HBE cells was 0.3%–13% following exposure to 10–10^5 CFU/mL *P. aeruginosa*. The relative maximum ROSs release was in Beas-2B cells, increased by 124.5% with exposure of 10^5 CFU/mL bacteria (Figures 3C and S2). The relative MMP ratio of cells from top to bottom of respiratory tract decreased by 5.5%–83.2%, 47.1%–90.3%, 17.5%–93.8%, and 19.5%–89.7%, respectively (Figures 3D and S3). Overall, *P. aeruginosa* induced the highest degree of mitochondrial depolarization in NP69 cells among these cell lines, leading to a greater reduction in the cellular proliferation activity. The changes of mitochondrial ROSs and MMP not only explain proliferation inhibition phenomenon within 6 h, but also provide key

https://doi.org/10.1021/envhealth.5c00063
Environ. Health XXXX, XXX, XXX–XXX

upstream triggers for the next stage of "inflammatory effect", reflecting continuity of "early injury-late response" during infection.

3.3.2. Pathogenic-Bacteria-Induced Cellular Inflammatory Effects. Damaged cells can activate innate immune response, which affects normal signal transduction, further triggering inflammation.[44] Therefore, we examined the levels of downstream proinflammatory cytokines and chemokines shared by NLRs and TLRs, including IL-6, IL-1β, TNF-α, and IL-8. The standard curves of the four cytokines with $R^2 > 99\%$ (Figures S4A−S4D) indicate reliability of experimental results. All respiratory tract cells secreted IL-6 and IL-1β during bacteria exposure (see Figures 3E and 3F), indicating that bacteria induce an inflammatory response in these cells. After exposure to 10−10^5 CFU/mL *P. aeruginosa*, the IL-6 level increased by 0%−136.0%, 14.5%−181.0%, 34.9%−157.6%, and 29.2%−62.2%, and the IL-1β level increased by 3.5%−135.3%, 50.2%−238.2%, 23.7%−180.5%, and 54.4%−159.0% in HNEpC, NP69, 16HBE, and Beas-2B cells, respectively. Therefore, *P. aeruginosa* was most likely to induce the production of IL-6 and IL-1β in NP69 cells, followed by 16HBE cells. The TNF-α secretion maintained at high levels in all cell lines under a relatively high bacteria exposure concentration (10^5 CFU/mL) (Figure 3G). The relative increase of TNF-α was the highest in HNEpC cells (50.4%−606.8%), followed by 16HBE cells (3.7%−180.4%) under exposure of 10−10^5 CFU/mL bacteria. Collectively, *P. aeruginosa* induced the severest inflammatory effects in NP69 cells by promoting the production of IL-6 and IL-1β. The mediation factors of inflammatory effect showed a cell-specific pattern in which NP69, 16HBE, and Beas-2B cells mediated inflammation through IL-6 and IL-1β, whereas HNEpC cells mainly mediated inflammation through TNF-α.

Chemokines trigger the recruitment of immune cells including leukocytes to sites of inflammation as part of the pathogen clearance mechanism.[47,48] Therefore, the IL-8 levels in respiratory tract cells were measured. The IL-8 production in the supernatant of HNEpC, 16HBE, and Beas-2B cells increased by 10.1%−30.9%, 21.2%−90.8%, and 6.6%−64.7%, respectively, with the highest being observed in NP69 cells (17.1%−385.7%) (Figure 3H). These indicate that *P. aeruginosa* induces NP69 cells to secrete the highest level of IL-8, which will, in turn, drive leukocytes to the inflammation site to clear bacteria.

It is beneficial to develop an appropriate inflammatory response against pathogen infection, but exacerbation or dysregulation of inflammatory response can cause an "inflammatory cytokine storm" that leads to more severe and long-lasting cell damage.[49,50] Based on the cell activity decrease (Figure 3A), these cells did exhibit an excessive inflammatory immune response during bacteria exposure and infection. Different respiratory epithelial cell types promoted diverse cytokines to exercise the function of inflammatory immunity.

3.3.3. NLR Signaling Pathway Mediates Bacteria-Induced Inflammation. Since we found that NLRs family members were more strongly expressed than TLRs family members upon *P. aeruginosa* exposure, gene expression in NLR signaling pathway were selected to explore intermediate molecular regulatory networks of primary recognition receptors and terminal inflammatory effect. Based on the NLR signaling pathway cascade in the Kyoto Encyclopedia of Genes and Genomes (Figure S5), the schematic diagram of signaling pathway and expression levels of the corresponding genes was produced (see Figures 4A and 4B). The four cell lines were bound to bacteria by up-regulating *NOD1* and *NOD2* expression, thereby transmitting signals to regulate cell death-induced kinase (RIPK2).[51] The greatest amplitude of up-regulated expression of *RIPK2* was observed in NP69 cells, by increasing 1.3 and 1.4 times ($p < 0.05$) following exposure to 10^3 and 10^5 CFU/mL bacteria, respectively. These indicate that NP69 cells activate their own enzymes to fight against bacterial infection. Furthermore, part of signals are transmitted by complexes encoded by Nemo and CHUK in the nuclear factor-kappa B (NF-κB) signaling pathway, while the other part is transmitted by complexes encoded by TAK1 and TAB along mitogen-activated protein kinase (MAPK) signaling pathway through JUN, and finally the signals are transmitted to nuclear DNA.[52] The majority of these intermediate domain genes up-regulated in NP69, 16HBE, and Beas-2B cells, with the highest being observed in NP69 cells, suggesting that NP69 cells may transmit the strongest bacterial signals to nuclear DNA via NF-κB and MAPK signaling pathways. After receiving the signal, the nuclear DNA of NP69 cells further induces proinflammatory, chemotactic, and antimicrobial peptide effects at the terminal.[53] Among the pro-inflammatory regulatory genes, *TNF-α* in NP69 cells up-regulated the greatest (3.4 and 271.8 times) after exposure to 10^3 and 10^5 CFU/mL bacteria, respectively. Furthermore, *IL-6* and *IL-18* expression increased to the greatest extent in NP69 cells, by 4.9- and 1.3-fold ($p < 0.01$), respectively, following exposure to 10^3 CFU/mL bacteria. When exposed to 10^5 CFU/mL bacteria, *IL-1β* up-regulated by 5.7, 6.9, 2.9, and 12.7 times ($p < 0.001$) in HNEpC, NP69, 16HBE, and Beas-2B cells, respectively. These suggest that *P. aeruginosa* induced a significant pro-inflammatory effect in all respiratory cells, consistent with the increased expression of the translated protein products IL-6, IL-1β, and TNF-α (see Figures 3E−G). Among chemotactic regulatory genes, the greatest upregulations of *IL-8* (5.6 times) and *CCL5* (1.9 times) were also in NP69 cells after exposure to 10^3 CFU/mL bacteria. The NP69 cells showed the greatest up-regulation of *CCL2* (11.1-fold) and *GRO* (2.6-fold) among these cell lines after exposure to 10^5 CFU/mL bacteria. With genes regulating antimicrobial peptides, *CAMP* up-regulated by 1.3 times ($p < 0.01$) in NP69 cells after exposure to 10^3 CFU/mL bacteria. Expression of *DEFB4* up-regulated by 1.8- and 6.1-time after exposure to 10^3 and 10^5 CFU/mL bacteria, respectively, with NP69 cells again representing the highest degree of up-regulation among these cell types. These show that the NP69 cells have the strongest inflammatory induction response after bacterial exposure, which is largely mediated by the NLR signaling pathway.

To further validate that the NLR signaling pathway mediates bacteria-induced inflammation, we screened key proteins in this pathway and examined their direct activation and phosphorylation status. The protein bands (Figure 4C) were normalized to relative expression levels (Figure 4D). The receptor protein NOD1 in NP69 cells up-regulated by 2.0- and 1.3-fold following exposure to 10^3 and 10^5 CFU/mL bacteria, respectively, whereas it down-regulated in other cell lines, indicating that initiation of the NOD-like receptor signaling pathway in NP69 cells was activated. Along the signaling pathway, following exposure to 10^3 CFU/mL bacteria, p-RIPK2 protein up-regulated by 1.8-, 2.2-, and 1.3-fold in HNEpC, NP69, and 16HBE cells, respectively, whereas it down-regulated by 67.9% in Beas-2B cells (Figures 4D and 4E). These indicate that the downstream key adapter protein

https://doi.org/10.1021/envhealth.5c00063
Environ. Health XXXX, XXX, XXX−XXX

RIPK2 underwent phosphorylation. Adapter molecules further transduced bacterial signals to the downstream pathway. Following exposure to 10^3 and 10^5 CFU/mL bacteria, downstream p-NF-κB protein (Figures 4D and 4F) in NP69 cells most significantly up-regulated among the four cell lines, with expression levels increased by 1.6- and 1.4-fold ($p < 0.05$), respectively. Combined with secretion of pro-inflammatory cytokines (IL-6, IL-1β, TNF-α) and chemokines (IL-8) (Figure 3), bacteria activated the NOD receptor signaling pathway at the initiation stage, through intermediate adapter molecules, to the terminal inflammatory responses. Thus, the NLR signaling pathway mediates bacteria-induced inflammation.

Therefore, when bacteria spread to the cellular surface, the bacterial cell wall can more easily bind to intracellular receptors of respiratory cells, and corresponding signals are then transmitted to nuclear DNA through NF-κB and MAPK signaling pathways. After receiving signal from nuclear DNA, respiratory cells produce antimicrobial peptides to suppress bacterial infection, and cells enter an inflammatory immune state. Furthermore, chemokines are released to recruit immune cells to the inflammatory site to further help defend against bacterial infection. Generally, the NLR signaling pathway is responsible for detecting and delivering bacterial signals and generating an inflammatory immune response. After bacterial exposure, the NP69 cells induced the strongest inflammatory immune response, compared to other cell types tested.

3.3.4. Inflammatory Epithelial Cells May Undergo Malignant Transformation. Cells undergoing inflammation tend to develop into fibrocytes and malignant tumor cells, and the likelihood of tumor cell development can be measured by epithelial-mesenchymal transition (EMT).[54,55] As a marker of malignant tumors,[56,57] the *β-catenin* gene down-regulated by 0.8 times and up-regulated by 1.6, 1.7, and 1.4 times for HNEpC, NP69, 16HBE, and Beas-2B cells, respectively, after exposure to 10^5 CFU/mL bacteria (Figure S6A). In addition, *Snail1* up-regulated by 1.8, 2.1, and 6.2 times and down-regulated by 0.7 times with exposure to 10^5 CFU/mL bacteria (Figure S6B). These indicate that NP69 and 16HBE cells are the most likely cells in the respiratory tract to develop into malignant tumor cells. Additionally, *Snail2* up-regulated by 3.1, 1.8, 1.5, and 1.2 times in HNEpC, NP69,16HBE, and Beas-2B cells, respectively, after exposure to 10^3 CFU/mL bacteria (Figure S6C), and *Vimentin*, respectively, up-regulated by 5.4, 2.4, 3.2, and 1.3 times with exposure to higher concentrations (10^5 CFU/mL) (Figure S6D). Other markers of mesenchymal transformation, including *β-catenin* and *FSP-1*, also up-regulated in all cells (Figures S6E and S6F).

Furthermore, the protein expression levels of N-cadherin (mesenchymal cadherin) and Vimentin (mesenchymal marker) were examined in respiratory tract cells (Figure S7). N-cadherin expression levels in HNEpC, NP69, and Beas-2B cells up-regulated by 1.7-, 2.3-, and 1.7-fold, respectively, after exposure to 10^5 CFU/mL bacteria, whereas they down-regulated by 21.8% in 16HBE cells. Additionally, Vimentin protein expression up-regulated by 1.2-, 1.3-, and 1.2-fold in HNEpC, NP69, and Beas-2B cells, respectively, following exposure to 10^3 CFU/mL bacteria, with a 10.8% reduction in 16HBE cells. Notably, NP69 cells displayed the most pronounced up-regulation of both EMT markers, directly confirming the EMT occurrence.

To further verify whether EMT is accompanied by enhanced malignant phenotypes (e.g., increased migratory capacity), wound healing experiments were conducted (Figure S8). At 6 h post-scratch, the scratch migration rates of NP69 and 6HBE cells increased by 1.1−1.8 folds and 0.6−1.1 folds, respectively, upon exposure to 10−10^3 CFU/mL, whereas they decreased at 10^4−10^5 CFU/mL exposure. The enhanced active migration capacity under low concentrations supports the central hypothesis that the EMT may drive malignant transformation. The changes in EMT markers at protein level and enhancement of functional phenotype (migration ability) provide preliminary evidence supporting the potential role of *P. aeruginosa* in promoting cell malignant transformation through inducing EMT. A definitive conclusion cannot be drawn, and further experiments are needed would help. Specifically, the nasopharynx and bronchus were the sites most susceptible to this series of pathological reactions. As an opportunistic pathogen, *P. aeruginosa* aggravates the course of respiratory disease[58,59] and induces further pathological changes.

Collectively, the results demonstrate that *P. aeruginosa* targets, adheres to, and spreads into NP69 cells, where they bind to cellular receptors and further induce inflammatory effects. Therefore, the Pearson correlation was analyzed to compare associations of various indicators in these cells (Table 1). With increasing exposure bacterial concentration, the amount of adhesion and invasion of bacteria as well as proliferation activity of these tested cells were significantly positively correlated, indicating that *P. aeruginosa* exerts statistically significant effects to these cells for three separate toxicity indices. Furthermore, we found significant correlations in MMP, IL-6, IL-1β, and IL-8 expression in NP69 cells, and in MMP and TNF-α expression in 16HBE cells. No significant correlation existed in other toxicity indices between HNEpC and Beas-2B cells. These indicate exposure to *P. aeruginosa* leading to more significant toxic effect on NP69 than 16HBE cells, confirming that *P. aeruginosa* is likely to preferentially attack NP69 cells to induce toxicity, followed by 16HBE cells. Even in high-exposure environments such as landfills, the bacterial concentration reaches a maximum order of magnitude of 10^5 CFU/m^3,[60] which is far lower than the experimental levels (10−10^5 CFU/mL). However, the concentration of *P. aeruginosa* in the sputum of cystic fibrosis patients can reach up to 10^5−10^9 CFU/mL,[61] indicating that the inhaled *P. aeruginosa* accumulates in the respiratory tract of susceptible populations (such as immunocompromised individuals), which poses a serious threat to their respiratory health.

Table 1. Correlation Analysis between Cytotoxicity Index and Cell Type

	HNEpC	NP69	16HBE	Beas-2B
adhesion	0.963**	0.937**	0.878*	0.913*
invasion	0.943**	0.987**	0.992**	0.975**
proliferation	0.839*	0.880*	0.822*	0.871*
ROS	0.651	−0.352	0.062	0.723
MMP	−0.699	−0.871*	−0.886*	−0.805
IL6	0.313	0.880*	0.537	0.545
IL1β	0.438	0.872*	0.223	0.137
TNFα	0.763	0.256	0.882*	0.483
IL8	−0.454	0.881*	0.169	−0.230

3.4. Mechanism of Respiratory Cytotoxicity of *P. aeruginosa*

Based on the above results, the process of top-down respiratory epithelial cells exposure and infection with *P. aeruginosa* can be

https://doi.org/10.1021/envhealth.5c00063
Environ. Health XXXX, XXX, XXX−XXX

divided into three steps: bacterial adhesion and transmission into the intracellular space, bacteria binding to host cellular receptors, and inflammatory toxicity (Figure 5). First, bacteria

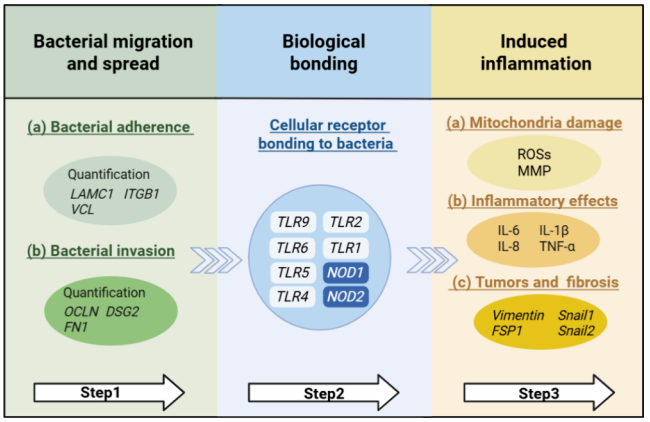

Figure 5. Proposed cytotoxicity mechanism of respiratory epithelial cells under *P. aeruginosa* exposure.

adhere to and spread to the surface of respiratory tract cells, and then bacteria on the surface break through epithelial cell barrier and further invade and spread to the interior of cells. Subsequently, host cells activate their intracellular NLRs (NOD1 and NOD2) to specifically recognize and bind to the cell wall of *P. aeruginosa*. Cellular receptors receive bacterial signal and activate NLR signaling pathway. Further targeting MMP results in decreasing or increasing ROSs accumulation in different human respiratory tract cells to induce mitochondrial damage. Finally, as a self-protective response, respiratory tract cells secrete plenty of pro-inflammatory factors to promote an inflammatory effect. This inflammatory response, in turn, promotes the secretion of chemokines, which tend to activate inflammatory immune cells to help fight infection and relieve inflammation. However, if further aggravated, inflammatory response potentially triggers malignant transformation of epithelial cells. Taken together, these results provide insight into the detailed mechanisms by which pathogenic bacteria induce cytotoxicity in respiratory tract cells. Among the four respiratory cells, NP69 cells were preferentially targeted by *P. aeruginosa* during exposure and infection of human respiratory epithelial cells.

4. CONCLUSIONS

A typical respiratory pathogen *P. aeruginosa* was used as a bacteria model to reveal the entire process of pathogen exposure and infection to four respiratory epithelial cells based on characteristics of bacterial intracellular transmission, bacteria binding to cellular receptors, and cytotoxic effects. *P. aeruginosa* tends to mainly transmit to the surface of NP69 cells and then further spread to the interior of cells. That is, NP69 cells are the preferential target of *P. aeruginosa*, whereas HNEpC cells show the lowest susceptibility to infection throughout the respiratory tract. Moreover, cell walls of *P. aeruginosa* are more easily recognized and bound by NP69 cells to activate the intracellular NLR signaling pathway. Thus, bacteria further induce a reduction of cellular proliferation activity, along with mitochondrial dysfunction and inflammatory effects, consequently activating immune cells to resist infection. Considering the entire process of bacteria exposure and infection, higher bacteria concentration induces stronger inflammatory damage to NP69 cells. Finally, NP69 cells in an inflammatory state may potentially undergo malignant transformation. Therefore, these results elucidate the interaction mechanism between *P. aeruginosa* and respiratory epithelial cells, providing a reference for a control strategy to reduce bacteria concentration or their transmission. From the perspective of diagnosis and treatment of respiratory diseases, these results further provide guidance for developing drugs targeting key genes in the related signaling pathways. However, further studies are still needed to clearly understand the exposure of bioaerosols in the environment, because there are fungi, viruses, organic matter, and other components in the environment. Additionally, future studies should employ an air−liquid interface exposure system to validate the toxicity results.

■ ASSOCIATED CONTENT

Supporting Information

The Supporting Information is available free of charge at https://pubs.acs.org/doi/10.1021/envhealth.5c00063.

Detailed information on materials and methods, Tables S1 and S2, and Figures S1−S8 (PDF)

■ AUTHOR INFORMATION

Corresponding Author

Taicheng An − *Guangdong-Hong Kong-Macao Joint Laboratory for Contaminants Exposure and Health, Guangdong Key Laboratory of Environmental Catalysis and Health Risk Control, Institute of Environmental Health and Pollution Control, Guangdong University of Technology, Guangzhou 510006, China; Guangzhou Key Laboratory of Environmental Catalysis and Pollution Control, Guangdong Basic Research Center of Excellence for Ecological Security and Green Development, School of Environmental Science and Engineering, Guangdong University of Technology, Guangzhou 510006, China;* orcid.org/0000-0001-6918-8070; Email: antc99@gdut.edu.cn

Authors

Caiqing Peng − *Guangdong-Hong Kong-Macao Joint Laboratory for Contaminants Exposure and Health, Guangdong Key Laboratory of Environmental Catalysis and Health Risk Control, Institute of Environmental Health and Pollution Control, Guangdong University of Technology, Guangzhou 510006, China; Guangzhou Key Laboratory of Environmental Catalysis and Pollution Control, Guangdong Basic Research Center of Excellence for Ecological Security and Green Development, School of Environmental Science and Engineering, Guangdong University of Technology, Guangzhou 510006, China*

Guiying Li − *Guangdong-Hong Kong-Macao Joint Laboratory for Contaminants Exposure and Health, Guangdong Key Laboratory of Environmental Catalysis and Health Risk Control, Institute of Environmental Health and Pollution Control, Guangdong University of Technology, Guangzhou 510006, China; Guangzhou Key Laboratory of Environmental Catalysis and Pollution Control, Guangdong Basic Research Center of Excellence for Ecological Security and Green Development, School of Environmental Science and Engineering, Guangdong University of Technology, Guangzhou 510006, China;* orcid.org/0000-0002-6777-4786

https://doi.org/10.1021/envhealth.5c00063
Environ. Health XXXX, XXX, XXX−XXX

Linghui Peng − *Guangdong-Hong Kong-Macao Joint Laboratory for Contaminants Exposure and Health, Guangdong Key Laboratory of Environmental Catalysis and Health Risk Control, Institute of Environmental Health and Pollution Control, Guangdong University of Technology, Guangzhou 510006, China; Guangzhou Key Laboratory of Environmental Catalysis and Pollution Control, Guangdong Basic Research Center of Excellence for Ecological Security and Green Development, School of Environmental Science and Engineering, Guangdong University of Technology, Guangzhou 510006, China*

Xi Fu − *Guangdong Provincial Engineering Research Center of Public Health Detection and Assessment, NMPA Key Laboratory for Technology Research and Evaluation of Pharmacovigilance, School of Public Health, Guangdong Pharmaceutical University, Guangzhou 510545, China*

Complete contact information is available at: https://pubs.acs.org/10.1021/envhealth.5c00063

Notes

The authors declare no competing financial interest.

■ ACKNOWLEDGMENTS

This work was supported by National Key Research and Development Project (No. 2023YFC3708204), and National Natural Science Foundation of China (Nos. U1901210 and 42177410).

■ REFERENCES

(1) Walser, S. M.; Gerstner, D. G.; Brenner, B.; Bunger, J.; Eikmann, T.; Janssen, B.; Kolb, S.; Kolk, A.; Nowak, D.; Raulf, M.; Sagunski, H.; Sedlmaier, N.; Suchenwirth, R.; Wiesmuller, G.; Wollin, K. M.; Tesseraux, I.; Herr, C. E. Evaluation of exposure-response relationships for health effects of microbial bioaerosols - A systematic review. *Int. J. Hyg. Environ. Health* **2015**, *218* (7), 577−589.

(2) Joung, Y. S.; Ge, Z.; Buie, C. R. Bioaerosol generation by raindrops on soil. *Nat. Commun.* **2017**, *8* (1), 14668.

(3) Zhao, J.; Jin, L.; Wu, D.; Xie, J.; Li, J.; Fu, X.; Cong, Z.; Fu, P.; Zhang, Y.; Luo, X.; et al. Global airborne bacterial community—interactions with Earth's microbiomes and anthropogenic activities. *Proc. Natl. Acad. Sci. U S A* **2022**, *119* (42), e2204465119.

(4) Zhang, Y.; Shen, F. X.; Yang, Y.; Niu, M. T.; Chen, D.; Chen, L. F.; Wang, S. Q.; Zheng, Y. H.; Sun, Y.; Zhou, F.; Qian, H.; Wu, Y.; Zhu, T. L. Insights into the profile of the human expiratory microbiota and its associations with indoor microbiotas. *Environ. Sci. Technol.* **2022**, *56* (10), 6282−6293.

(5) Dai, R. C.; Liu, S.; Li, Q. S.; Wu, H. T.; Wu, L.; Ji, C. H. A systematic review and meta-analysis of indoor bioaerosols in hospitals: The influence of heating, ventilation, and air conditioning. *PLoS One* **2021**, *16* (12), e0259996.

(6) Zhang, T.; Chen, Y.; Cai, Y.; Yu, Y.; Liu, J.; Shen, X.; Li, G.; An, T. Abundance and cultivable bioaerosol transport from a municipal solid waste landfill area and its risks. *Environ. Pollut.* **2023**, *320*, No. 121038.

(7) Gordon, S. B.; Bruce, N. G.; Grigg, J.; Hibberd, P. L.; Kurmi, O. P.; Lam, K. B. H.; Mortimer, K.; Asante, K. P.; Balakrishnan, K.; Balmes, J.; Bar-Zeev, N.; Bates, M. N.; Breysse, P. N.; Buist, S.; Chen, Z. M.; Havens, D.; Jack, D.; Jindal, S.; Kan, H. D.; Mehta, S.; Moschovis, P.; Naeher, L.; Patel, A.; Perez-Padilla, R.; Pope, D.; Rylance, J.; Semple, S.; Martin, W. J. Respiratory risks from household air pollution in low and middle income countries. *Lancet Respir. Med.* **2014**, *2* (10), 823−860.

(8) Priyamvada, H.; Singh, R. K.; Akila, M.; Ravikrishna, R.; Verma, R. S.; Gunthe, S. S. Seasonal variation of the dominant allergenic fungal aerosols - One year study from southern Indian region. *Sci. Rep.* **2017**, *7* (1), 11171.

(9) Raymenants, J.; Geenen, C.; Budts, L.; Thibaut, J.; Thijssen, M.; De Mulder, H.; Gorissen, S.; Craessaerts, B.; Laenen, L.; Beuselinck, K.; et al. Indoor air surveillance and factors associated with respiratory pathogen detection in community settings in Belgium. *Nat. Commun.* **2023**, *14* (1), 1332.

(10) Zhang, X.; Lu, B.; Yang, S.; Lin, B.; Chen, G.; Wang, L.; Peng, Z.; Lu, H.; Wang, C.; Li, D.; Chen, J. Characterization and health risk assessment of airborne fungi in a semiunderground municipal wastewater treatment plant. *Environ. Health* **2025**, *3* (3), 227−237.

(11) Ma, J.; Wang, M.; Sun, Y.; Zheng, Y.; Lai, S.; Zhang, Y.; Wu, Y.; Jiang, C.; Shen, F. Cockroach microbiome disrupts indoor environmental microbial ecology with potential public health implications. *Environ. Health* **2025**, *3* (4), 380−391.

(12) Finch, S.; McDonnell, M. J.; Abo-Leyah, H.; Aliberti, S.; Chalmers, J. D. A comprehensive analysis of the impact of *Pseudomonas aeruginosa* colonization on prognosis in adult bronchiectasis. *Ann. Am. Thorac. Soc.* **2015**, *12* (11), 1602−1611.

(13) Garau, J.; Gomez, L. P*seudomonas aeruginosa* pneumonia. *Curr. Opin. Infect. Dis.* **2003**, *16* (2), 135−143.

(14) Eklöf, J.; Misiakou, M. A.; Sivapalan, P.; Armbruster, K.; Browatzki, A.; Nielsen, T. L.; Lapperre, T. S.; Andreassen, H. F.; Janner, J.; Ulrik, C. S.; Gabrielaite, M.; Johansen, H. K.; Jensen, A.; Nielsen, T. V.; Hertz, F. B.; Ghathian, K.; Calum, H.; Wilcke, T.; Seersholm, N.; Jensen, J.-U. S.; Marvig, R. L. Persistence and genetic adaptation of *Pseudomonas aeruginosa* in patients with chronic obstructive pulmonary disease. *Clin. Microbiol. Infect.* **2022**, *28* (7), 990−995.

(15) Langan, K. M.; Kotsimbos, T.; Peleg, A. Y. Managing Pseudomonas aeruginosa respiratory infections in cystic fibrosis. *Curr. Opin. Infect. Dis.* **2015**, *28* (6), 547−556.

(16) Man, W. H.; de Steenhuijsen Piters, W. A.; Bogaert, D. The microbiota of the respiratory tract: gatekeeper to respiratory health. *Nat. Rev. Microbiol.* **2017**, *15* (5), 259−270.

(17) Wu, Y.; Wang, Y.; Yang, H.; Li, Q.; Gong, X.; Zhang, G.; Zhu, K. Resident bacteria contribute to opportunistic infections of the respiratory tract. *PLoS Pathog.* **2021**, *17* (3), e1009436.

(18) Grimwood, K.; Kyd, J. M.; Owen, S. J.; Massa, H. M.; Cripps, A. W. Vaccination against respiratory *Pseudomonas aeruginosa* infection. *Hum. Vaccin. Immunother.* **2015**, *11* (1), 14−20.

(19) Li, Q.; Pan, C.; Teng, D.; Lin, L.; Kou, Y.; Haase, E. M.; Scannapieco, F. A.; Pan, Y. Porphyromonas gingivalis modulates *Pseudomonas aeruginosa*-induced apoptosis of respiratory epithelial cells through the STAT3 signaling pathway. *Microbes Infect.* **2014**, *16* (1), 17−27.

(20) Cigana, C.; Bianconi, I.; Baldan, R.; De Simone, M.; Riva, C.; Sipione, B.; Rossi, G.; Cirillo, D. M.; Bragonzi, A. *Staphylococcus aureus* impacts *Pseudomonas aeruginosa* chronic respiratory disease in murine models. *J. Infect. Dis.* **2018**, *217* (6), 933−942.

(21) Thomas, R. J. Particle size and pathogenicity in the respiratory tract. *Virulence* **2013**, *4* (8), 847−858.

(22) Fröhlich-Nowoisky, J.; Kampf, C. J.; Weber, B.; Huffman, J. A.; Pöhlker, C.; Andreae, M. O.; Lang-Yona, N.; Burrows, S. M.; Gunthe, S. S.; Elbert, W.; Su, H.; Hoor, P.; Thines, E.; Hoffmann, T.; Després, V. R.; Pöschl, U. Bioaerosols in the Earth system: Climate, health, and ecosystem interactions. *Atmos. Res.* **2016**, *182*, 346−376.

(23) Guo, Y.; Wei, J. J.; Ou, C. Y.; Liu, L.; Sadrizadeh, S.; Jin, T.; Tang, L. L.; Zhang, Y. P.; Li, Y. G. Deposition of droplets from the trachea or bronchus in the respiratory tract during exhalation: A steady-state numerical investigation. *Aerosol Sci. Technol.* **2020**, *54* (8), 869−879.

(24) Chang, C. W.; Li, S. Y.; Huang, S. H.; Huang, C. K.; Chen, Y. Y.; Chen, C. C. Effects of ultraviolet germicidal irradiation and swirling motion on airborne *Staphylococcus aureus, Pseudomonas aeruginosa* and *Legionella pneumophila* under various relative humidities. *Indoor Air* **2013**, *23* (1), 74−84.

(25) Kalwasinska, A.; Burkowska, A.; Swiontek Brzezinska, M. Exposure of workers of municipal landfill site to bacterial and fungal aerosol. *Clean-Soil Air Water* **2014**, *42* (10), 1337−1343.
(26) Han, Y. P.; Yang, T.; Yan, X.; Li, L.; Liu, J. X. Effect of aeration mode on aerosol characteristics from the same wastewater treatment plant. *Water Res.* **2020**, *170*, No. 115324.
(27) Aliskan, H.; Colakoglu, S.; Turunç, T.; Demiroglu, Y. Z.; Erdogan, F.; Akin, S.; Arslan, H. Four years monitorization of antibiotic sensitivity rates of *Pseudomonas aeruginosa* and *Acinetobacter baumannii* strains isolated from patients in intensive care unit and inpatient clinics. *Mikrobiyol. Bul.* **2008**, *42* (2), 321−329.
(28) Wang, Y. J.; Zhang, S.; Li, L.; Zhang, Q.; Yang, L. Y.; Yang, K.; Liu, Y.; Zhu, H. R.; Lai, B. S.; Wu, J.; Hua, L. L. Airborne ARGs/ MGEs from two sewage types during the COVID-21: Population, microbe interactions, cytotoxicity, formation mechanism, and dispersion. *Water Res.* **2024**, *254*, No. 121368.
(29) Wang, Y. J.; Yang, K.; Li, L.; Yang, L. Y.; Zhang, S.; Yu, F. F.; Hua, L. L. Change characteristics, bacteria host, and spread risks of bioaerosol ARGs/ MGEs from different stages in sewage and sludge treatment process. *J. Hazard. Mater.* **2024**, *469*, No. 134011.
(30) Lamari, F.; Chakroun, I.; Rtimi, S. Assessment of the correlation among antibiotic resistance, adherence to abiotic and biotic surfaces, invasion and cytotoxicity of Pseudomonas aeruginosa isolated from diseased gilthead sea bream. *Colloids Surf. B-Biointerfaces* **2017**, *158*, 229−236.
(31) Priolli, D. G.; Abrantes, A. M.; Neves, S.; Goncalves, A. C.; Lopes, C. O.; Martinez, N. P.; Cardinalli, I. A.; Sarmento Ribeiro, A. B.; Botelho, M. F. Microenvironment influence on human colon adenocarcinoma phenotypes and matrix metalloproteinase-2, p53 and beta-catenin tumor expressions from identical monoclonal cell tumor in the orthotopic model in athymic nude rats. *Scand. J. Gastroenterol.* **2014**, *49* (3), 309−316.
(32) Klemm, P.; Vejborg, R. M.; Hancock, V. Prevention of bacterial adhesion. *Appl. Microbiol. Biotechnol.* **2010**, *88* (2), 451−459.
(33) Feng, Y.; Wang, S.; Liu, X.; Han, Y.; Xu, H.; Duan, X.; Xie, W.; Tian, Z.; Yuan, Z.; Wan, Z.; et al. Geometric constraint-triggered collagen expression mediates bacterial-host adhesion. *Nat. Commun.* **2023**, *14* (1), 8165.
(34) Bialer, M. G.; Sycz, G.; Muñoz González, F.; Ferrero, M. C.; Baldi, P. C.; Zorreguieta, A. Adhesins of Brucella: Their roles in the interaction with the host. *Pathogens* **2020**, *9* (11), 942.
(35) da Silva, C. V.; Cruz, L.; Araujo, N. D.; Angeloni, M. B.; Fonseca, B. B.; Gomes, A. D.; Carvalho, F. D.; Goncalves, A. L. R.; Barbosa, B. D. A glance at Listeria and Salmonella cell invasion: Different strategies to promote host actin polymerization. *Int. J. Med. Microbiol.* **2012**, *302* (1), 19−32.
(36) Barbara, G.; Barbaro, M. R.; Fuschi, D.; Palombo, M.; Falangone, F.; Cremon, C.; Marasco, G.; Stanghellini, V. Inflammatory and microbiota-related regulation of the intestinal epithelial barrier. *Front. Nutr.* **2021**, *8*, No. 718356.
(37) Horowitz, A.; Chanez-Paredes, S. D.; Haest, X.; Turner, J. R. Paracellular permeability and tight junction regulation in gut health and disease. *Nat. Rev. Gastroenterol. Hepatol.* **2023**, *20* (7), 417−432.
(38) Kanchanawong, P.; Calderwood, D. A. Organization, dynamics and mechanoregulation of integrin-mediated cell−ECM adhesions. *Nat. Rev. Mol. Cell Biol.* **2023**, *24* (2), 142−161.
(39) Antoni, L.; Nuding, S.; Wehkamp, J.; Stange, E. F. Intestinal barrier in inflammatory bowel disease. *World J. Gastroenterol.* **2014**, *20* (5), 1165−1179.
(40) Coillard, A.; Guyonnet, L.; De Juan, A.; Cros, A.; Segura, E. TLR or NOD receptor signaling skews monocyte fate decision via distinct mechanisms driven by mTOR and miR-155. *Proc. Natl. Acad. Sci. U S A* **2021**, *118* (43), No. e2109225118.
(41) Pashenkov, M. V.; Dagil, Y. A.; Pinegin, B. V. NOD1 and NOD2: Molecular targets in prevention and treatment of infectious diseases. *Int. Immunopharmacol.* **2018**, *54*, 385−400.
(42) Chamaillard, M.; Hashimoto, M.; Horie, Y.; Masumoto, J.; Qiu, S.; Saab, L.; Ogura, Y.; Kawasaki, A.; Fukase, K.; Kusumoto, S.; et al. An essential role for NOD1 in host recognition of bacterial peptidoglycan containing diaminopimelic acid. *Nat. Immunol.* **2003**, *4* (7), 702−707.
(43) Chuenchor, W.; Jin, T.; Ravilious, G.; Xiao, T. S. Structures of pattern recognition receptors reveal molecular mechanisms of autoinhibition, ligand recognition and oligomerization. *Curr. Opin. Immunol.* **2014**, *26*, 14−20.
(44) Li, D.; Wu, M. Pattern recognition receptors in health and diseases. *Signal Transduct. Target. Ther.* **2021**, *6* (1), 291.
(45) Gajewski, T. F.; Schreiber, H.; Fu, Y.-X. Innate and adaptive immune cells in the tumor microenvironment. *Nat. Immunol.* **2013**, *14* (10), 1014−1022.
(46) Lu, L.; Hu, J.; Li, G.; An, T. Low concentration Tetrabromobisphenol A (TBBPA) elevating overall metabolism by inducing activation of the Ras signaling pathway. *J. Hazard. Mater.* **2021**, *416*, No. 125797.
(47) Lisignoli, G.; Grassi, F.; Piacentini, A.; Cocchini, B.; Remiddi, G.; Bevilacqua, C.; Facchini, A. Hyaluronan does not affect cytokine and chemokine expression in osteoarthritic chondrocytes and synoviocytes. *Osteoarthritis Cartilage* **2001**, *9* (2), 161−168.
(48) Stojkovic, B.; McLoughlin, R. M.; Meade, K. G. In vivo relevance of polymorphic Interleukin 8 promoter haplotype for the systemic immune response to LPS in Holstein-Friesian calves. *Vet. Immunol. Immunopathol.* **2016**, *182*, 1−10.
(49) Tay, M. Z.; Poh, C. M.; Renia, L.; MacAry, P. A.; Ng, L. F. P. The trinity of COVID-19: immunity, inflammation and intervention. *Nat. Rev. Immunol.* **2020**, *20* (6), 363−374.
(50) Tan, L. Y.; Komarasamy, T. V.; Rmt Balasubramaniam, V. Hyperinflammatory Immune Response and COVID-19: A Double Edged Sword. *Front. Immunol.* **2021**, *12*, 742941.
(51) You, J. Q.; Wang, Y.; Chen, H. F.; Jin, F. RIPK2: a promising target for cancer treatment. *Front. Pharmacol.* **2023**, *14*, 1192970.
(52) Hofmann, S. R.; Girschick, L.; Stein, R.; Schulze, F. Immune modulating effects of receptor interacting protein 2 (RIP2) in autoinflammation and immunity. *Clin. Immunol.* **2021**, *223*, 108648.
(53) Kumar, S.; Ingle, H.; Prasad, D. V. R.; Kumar, H. Recognition of bacterial infection by innate immune sensors. *Crit. Rev. Microbiol.* **2013**, *39* (3), 229−246.
(54) Boros, E.; Nagy, I. The role of MicroRNAs upon epithelial-to-mesenchymal transition in inflammatory bowel disease. *Cells* **2019**, *8* (11), 1461.
(55) Distler, J. H. W.; Gyorfi, A. H.; Ramanujam, M.; Whitfield, M. L.; Konigshoff, M.; Lafyatis, R. Shared and distinct mechanisms of fibrosis. *Nat. Rev. Rheumatol.* **2019**, *15* (12), 705−730.
(56) Xu, C. R.; Xu, Z.; Zhang, Y.; Evert, M.; Calvisi, D. F.; Chen, X. *β*-Catenin signaling in hepatocellular carcinoma. *J. Clin. Invest.* **2022**, *132* (4), No. e154515.
(57) Murillo-Garzón, V.; Kypta, R. WNT signalling in prostate cancer. *Nat. Rev. Urol.* **2017**, *14* (11), 683−696.
(58) Qin, S.; Xiao, W.; Zhou, C.; Pu, Q.; Deng, X.; Lan, L.; Liang, H.; Song, X.; Wu, M. *Pseudomonas aeruginosa*: pathogenesis, virulence factors, antibiotic resistance, interaction with host, technology advances and emerging therapeutics. *Signal Transduct. Target. Ther.* **2022**, *7* (1), 199.
(59) Rossi, E.; La Rosa, R.; Bartell, J. A.; Marvig, R. L.; Haagensen, J. A. J.; Sommer, L. M.; Molin, S.; Johansen, H. K. *Pseudomonas aeruginosa* adaptation and evolution in patients with cystic fibrosis. *Nat. Rev. Microbiol.* **2021**, *19* (5), 331−342.
(60) Kalwasińska, A.; Burkowska, A.; Swiontek Brzezinska, M. Exposure of workers of municipal landfill site to bacterial and fungal aerosol. *CLEAN Soil, Air, Water* **2014**, *42* (10), 1337−1343.
(61) Hisert, K. B.; Heltshe, S. L.; Pope, C.; Jorth, P.; Wu, X.; Edwards, R. M.; Radey, M.; Accurso, F. J.; Wolter, D. J.; Cooke, G.; Adam, R. J.; Carter, S.; Grogan, B.; Launspach, J. L.; Donnelly, S. C.; Gallagher, C. G.; Bruce, J. E.; Stoltz, D. A.; Welsh, M. J.; Hoffman, L. R.; McKone, E. F.; Singh, P. K. Restoring cystic fibrosis transmembrane conductance regulator function reduces airway bacteria and inflammation in people with cystic fibrosis and chronic lung infections. *Am. J. Respir. Crit. Care Med.* **2017**, *195* (12), 1617−1628.

https://doi.org/10.1021/envhealth.5c00063
Environ. Health XXXX, XXX, XXX−XXX